Title
Diurnal cycle of the South Pacific Convergence Zone in 30 years of satellite images

Journal
Journal of Geophysical Research: Atmospheres, 120(18)

ISSN
2169-897X

Authors
Haffke, Colene
Magnusdottir, Gudrun

Publication Date
2015-09-27

DOI
10.1002/2015jd023436

AGU PUBLICATIONS

JGR

Journal of Geophysical Research: Atmospheres

RESEARCH ARTICLE
10.1002/2015JD023436

Key Points:
- Diurnal cycle of SPCZ area, mean IR, and cloud height
- Seasonal evolution of diurnal cycle
- Modulation of SPCZ diurnal cycle by ENSO and MJO

Correspondence to:
G. Magnusdottir,
gudrun@uci.edu

Citation:
Haffke, C., and G. Magnusdottir (2015), Diurnal cycle of the South Pacific Convergence Zone in 30 years of satellite images, *J. Geophys. Res. Atmos.*, *120*, 9059–9070, doi:10.1002/2015JD023436.

Received 1 APR 2015
Accepted 14 AUG 2015
Accepted article online 18 AUG 2015
Published online 17 SEP 2015

Diurnal cycle of the South Pacific Convergence Zone in 30 years of satellite images

Colene Haffke[1] and Gudrun Magnusdottir[1]

[1]Department of Earth System Science, University of California, Irvine, California, USA

Abstract A data set of three-hourly South Pacific Convergence Zone (SPCZ) location and extent, from which IR temperature within the SPCZ may be obtained, for 1980–2012, November–April is used to examine the diurnal cycle of the SPCZ. Maximum SPCZ area occurs at 15:00–18:00 local standard time (LST). Two minima in mean IR temperature are evident, one at 13:00–16:00 LST, nearly coinciding with the maximum in area, and the second in the early morning hours at 05:00–07:00 LST, when area is at a minimum. The morning minimum in mean IR temperature is associated with a peak in deep convection while the afternoon minimum is associated with a peak in midlevel clouds. On average, the morning minimum in IR temperature dominates in the tropical regions of the SPCZ, while the afternoon IR temperature minimum dominates in the subtropical regions of the SPCZ. The relative strength of the two IR temperature minima is affected by the seasonal cycle, intraseasonal variability associated with active Madden Julian Oscillation events, and interannual variability due to the El Niño Southern Oscillation. The morning IR temperature minimum becomes more dominant when the SPCZ is more frequently present or when the SPCZ is shifted toward the equator. In terms of cloud height, midlevel clouds dominate at all times in all regions of the SPCZ and peak in abundance between 15:00–18:00 LST. Low-level clouds peak near midnight and then transition to high-level clouds, which peak between 03:00–06:00 LST, just before sunrise.

1. Introduction

The South Pacific Convergence Zone (SPCZ) is an elongated convection zone that stretches from the equatorial region north of Australia poleward and eastward toward 30°S in the central Pacific [e.g., *Vincent*, 1994]. In a global context it is a major precipitating region, most active during the austral summer half-year from November to April.

Historically, in situ observations of the SPCZ have been scarce due to its remote location over the central Pacific Ocean. Satellites have provided a wealth of information since around 1980 through infrared (IR) and visible images from which cloud cover can be inferred. Recently, satellite observations have been used to greatly advance our knowledge of SPCZ behavior on a number of time scales. Our understanding of the interannual variability [*Folland et al.*, 2002; *Vincent et al.*, 2011; *Haffke and Magnusdottir*, 2013] and intraseasonal variability [*Haffke and Magnusdottir*, 2013] of the SPCZ has improved within the last decade. Hypothesis on SPCZ formation and maintenance have also emerged [*Takahashi and Battisti*, 2007; *Widlansky et al.*, 2011; *Matthews*, 2012].

The SPCZ has a diagonal tilt with the western part of the cloud band located in the tropics, while the eastern part is located in the subtropics. *Haffke and Magnusdottir* [2013] describe some of the major differences between the tropical and subtropical parts of the SPCZ. They find that the two parts of the SPCZ are oriented differently such that the subtropical part has a steeper slope. At times the two parts of the SPCZ are not connected at all. In the tropics deeper convection over a larger area is common compared to the subtropics. In the tropics, overall SPCZ activity, in terms of fraction of time present, reaches a maximum over the greatest area in January and SPCZ area peaks in early February whereas in the subtropics, area and activity peak earlier, in December. There is a stronger connection between SPCZ location and activity and the sea surface temperature (SST) distribution in the tropics than in the subtropics. The location of the SPCZ varies strongly interannually depending on El Niño–Southern Oscillation (ENSO) phase, so that during strong El Niño years the SPCZ tilts far less, and even the eastern part of the SPCZ takes on a tropical character. This is associated with the warm SST in the equatorial area at this time. However, *Haffke and Magnusdottir* [2013] find that ENSO does not affect the total area of the SPCZ. On the intraseasonal time scale, they find a distinct Madden Julian

Oscillation (MJO) signature in terms of location and area of the SPCZ. Examining the intraseasonal power spectrum of SPCZ area, *Haffke and Magnusdottir* [2013] found that the strongest signal in both sectors of the SPCZ was associated with the diurnal time scale (see their Figure 7). Yet in recent years relatively little has been discussed in the literature regarding shorter time scales such as the diurnal cycle compared to studies focusing on longer time scales. The current study focuses on diurnal variability of the SPCZ.

The diurnal cycle in cloudiness is forced by incoming solar radiation, which reaches peak intensity at local noon, and the maximum total heating that peaks in late afternoon. Over land, this often results in a direct response from convective clouds as instability reaches a maximum when the surface reaches maximum heating in late afternoon [*Meisner and Arkin*, 1987; *Yang and Slingo*, 2001; *Janowiak et al.*, 1994]. Over the ocean the relationship between the diurnal cycle of solar heating and maximum in cloud cover and deep convection is a bit more complicated. Maximum midlevel cloud cover tends to occur in the afternoon or early evening over the open ocean while maximum deep cloud coverage occurs in the early morning [e.g., *Yang and Slingo*, 2001]. One explanation for the morning maximum in deep clouds is due to a direct radiation-convection effect where afternoon convection is suppressed due to more solar radiation being absorbed by cloud tops, stabilizing the air and suppressing convection, while nighttime convection is enhanced as radiative cooling of cloud tops enhances instability and promotes convection [*Randall et al.*, 1991; *Yang and Slingo*, 2001]. Other theories highlight the importance of the organization of the cloud systems and suggest that the morning maximum is associated with a day versus night contrast between radiative cooling in the developed cloudy area and the surrounding cloud-free areas. [*Gray and Jacobson*, 1977; *Yang and Slingo*, 2001]. *Nesbitt and Zipser* [2003] argue that the morning maximum in precipitation rate is due to an increased number of mesoscale convective systems that are favored to grow and become long lived in the nighttime hours. Due to the conflicting theories and limited observations in the past, the processes controlling the diurnal cycle in cloudiness and rainfall over the ocean are less well understood than those over land. *Yang and Smith* [2006] eloquently summarize the various physical mechanisms that have been suggested as controlling the diurnal cycle of tropical precipitation. As pointed out in their paper, there are many possible mechanisms that may work in tandem.

Table 1 of *Bain et al.* [2010] presents an overview of some of the key results from several studies that have assessed the phase and amplitude of the diurnal cycle from observations over the tropical oceans. In terms of deep clouds and rainfall, most studies find an early morning peak and some also note an afternoon maximum in warmer clouds. Many of these studies are limited by the spatial resolution of the data using only surface station data, or by the time span of the data set. Two of the longest studies were conducted using 22 years of ship and surface station rainfall observations [*Dorman and Bourke*, 1979; *Dai*, 2001]. Satellite observations with higher spatial resolution often cover a shorter time span ranging from one month to 13 years [*Bain et al.*, 2010]. For example, *Yen* [2005] examined the diurnal cycle over the west Pacific from 1980 to 1993 using IR temperature. However, the area of study was limited to 15°S–45°N, excluding much of the subtropical SPCZ. Few studies have focused specifically on the diurnal cycle in the SPCZ.

Using GOES IR temperature satellite data from January to February 1979, *Albright et al.* [1985] define the SPCZ as the region where the average fractional cover of deep clouds (IR $<$ 237 K) is greater than 20%. They find a pronounced diurnal cycle in the fractional coverage of very deep clouds (IR $<$ 218 K) in the SPCZ region that deviated from the daily mean by as much as 60%, peaking in the early morning hours, between 03:00 and 06:00 local standard time (LST). In contrast, fractional coverage of deep clouds (IR $<$ 237 K) peaked in the afternoon or evening. *Albright et al.* [1985] also note differences between the western SPCZ (170°E–170°W) and eastern SPCZ (170°W–147°W) in the cloud types, precipitation amounts, and phase of the diurnal cycle, noting that the eastern SPCZ has a peak in the afternoon while the western Pacific peaks in the early evening around 21:00 LST. A study by *Nitta and Sekine* [1994] corroborate the double peak in the diurnal cycle of the SPCZ using a longer time series of IR satellite images (1980–1989), finding one in the early morning between 03:00 and 04:00 LST and one in the afternoon between 15:00 and 16:00 LST. In their study, the diurnal cycle of the SPCZ was analyzed at four latitudes (6.5°S, 8.5°S, 10.5°S, and 12.5°S) along 170.5°E, an area where clouds were, on average, colder than 250 K.

We will expand on these findings to fully describe the diurnal cycle of the entire SPCZ. Using a more sophisticated definition of SPCZ presence and extent [*Haffke and Magnusdottir*, 2013], we will describe the diurnal cycle of the entire SPCZ, including the subtropical portion, which has largely been ignored in previous studies

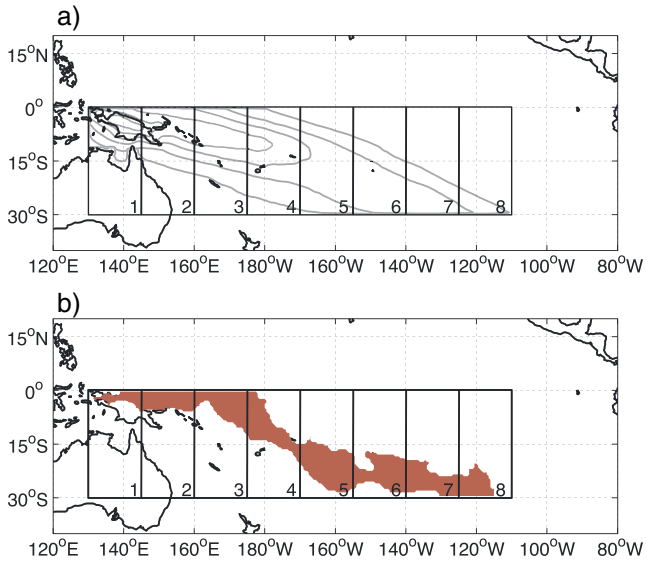

Figure 1. (a) The domain for this study is outlined above in the inner black box spanning 0–30°S, 130°E–110°W. Eight subregions are outlined in the smaller black boxes spanning 0–30°S in latitude and longitudinally as follows: (1) 130°E–145°E, (2) 145°E–160°E, (3) 160°E–175°E, (4) 175°E–170°W, (5) 170°W–155°W, (6) 155°W–140°W, (7) 140°W–125°W, and (8) 125°W–110°W. Subregions are used to correct for LST and to isolate different parts of the SPCZ to compare behavior. Gray contours in the top plot show a composite of all SPCZ labels, November–April 1980–2012 (excluding November 1987 to April 1989). Units are in fraction of time present starting at 10% in intervals of 10%. (b) An example of an SPCZ label is shown in the bottom plot from 28 November 2006 at 18Z.

due to generally warmer cloud tops. We will also address the impact of the seasonal cycle, intraseasonal variability in terms of the Madden Julian Oscillation (MJO), and variability related to the El Niño–Southern Oscillation (ENSO) on the diurnal cycle.

The paper is organized as follows: Section 2 describes the data set of SPCZ presence and identifies the IR data set from which it was obtained. These data will be used to investigate the diurnal cycle in area and cloud top height. Section 3 contains results, first in terms of the basic diurnal cycle in section 3.1. Next, the seasonal variations in the diurnal cycle are outlined in section 3.2. Sections 3.3 and 3.4 show how the diurnal cycle is affected by the MJO and ENSO, respectively. Concluding remarks are made in section 4.

2. Data

The geostationary satellite data used in this study come from the atmospheric window channel (IR) of the GridSat archive that is described in detail in *Knapp et al.* [2011] and has been used in a number of other climate studies. GridSat represents a collection of satellite images with global and long-term coverage, originating from the ISCCP B1 archive at 10 km spatial resolution every 3 h, but the images have been further processed, intercalibrated, and stitched together for the global coverage. *Haffke and Magnusdottir* [2013] created a set of SPCZ labels, defining the instantaneous location and area extent of the SPCZ every 3 h from 1980 to 2012 during November–April based on the raw data from GridSat that had been coarsened to 0.5° × 0.5° spatial resolution. The binary labels indicate SPCZ presence or absence at each 0.5° × 0.5° grid point in a domain extending from the equator to 30°S and from 130°E to 110°W. SPCZ labels are obtained from a Markov random field statistical model using the IR satellite images as input data. The spatiotemporal statistical model uses Bayesian statistics to determine the probability of the SPCZ being present or absent at each grid point. Built into the method is a recursive element since each grid point is more likely to be part of the SPCZ if neighboring grid points (in space and time) are parts of it. Thus, the model is designed to emulate the way a human observer would identify the SPCZ in a time series of satellite images. A full description of the model is found in *Bain et al.* [2011], and details of how the model is adapted for the SPCZ are found in *Haffke and Magnusdottir* [2013]. The SPCZ labels provide a valuable data set for this study because they describe the envelope of convection associated with the SPCZ, including any areas of clear sky that may be within the general area of cloudiness. This allows for the quantification of SPCZ area as well as quantities within the labels, such as IR temperature.

3. Results

Figure 1a shows the study domain and designates eight subregions to correct for local standard time (LST). Figure 1a also shows a composite mean of all SPCZ labels to indicate the mean location of the SPCZ over November–April 1980–2012. Figure 1b shows a single SPCZ label from 28 November 2006 at 18Z. The eight subregions will also be used to describe how the diurnal cycle is different along the length of the SPCZ. Numerous islands are located in the far west region, Region 1, resulting in a high proportion of land surface

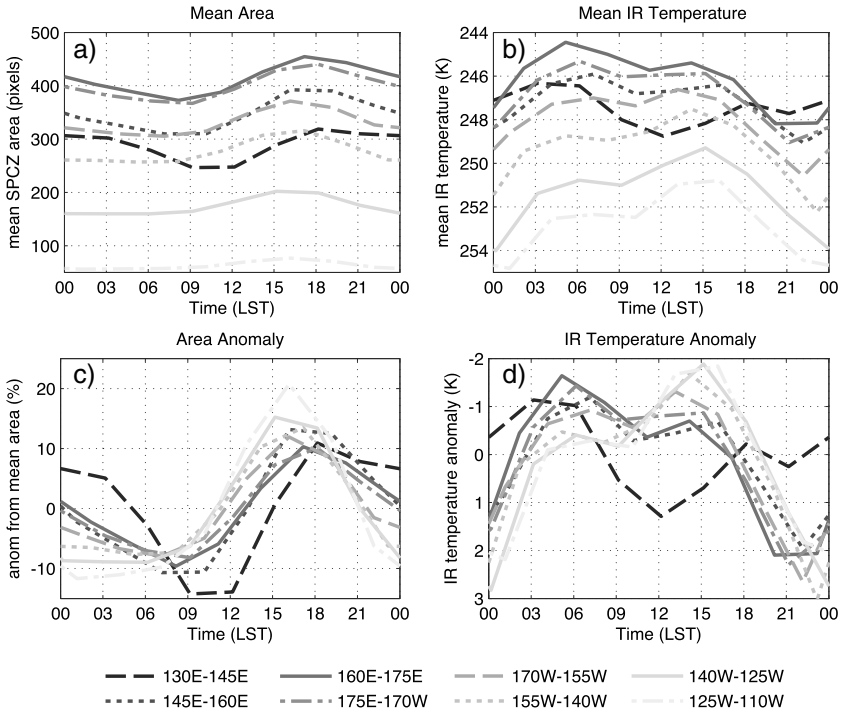

Figure 2. Diurnal cycle of SPCZ area and mean IR temperature for each region. The top row shows (a) mean SPCZ area (number of 0.5° pixels) and (b) mean IR temperature (K) (note the inverted scale), while the bottom row shows (c) anomalies from the regional mean for area (% change) and (d) from the mean IR temperature (K). All values have been corrected for LST.

and therefore different conditions that strongly affect the diurnal cycle of cloudiness and precipitation [e.g., *Teo et al.*, 2011].

In the following, the diurnal cycle will be described in terms of area, mean IR temperature, and fractional coverage of clouds at different heights. Area will be calculated as the total areal extent of the SPCZ label within a given region. Mean IR temperature will be calculated as the mean IR temperature within the SPCZ labels. Cloud height is estimated using IR temperatures. The percent coverage of different cloud heights will be based on the fraction of the SPCZ label covered by a certain range of IR temperature. Based on a similar method used in *Bain et al.* [2010] we have assigned a range of IR temperature values to four categories of clouds: high clouds ($IR < 220\,K$), midlevel clouds ($220\,K < IR < 255\,K$), low-level clouds ($255\,K < IR < 280\,K$), and clear sky ($IR > 280\,K$). Our results that are described below are statistically significant at the 95% level using *F* test.

3.1. Diurnal Cycle of SPCZ Area, Mean IR Temperature, and Cloud Top Height

The diurnal cycles of SPCZ area and mean IR temperature are shown in Figure 2 where the top row shows mean values for each region and the bottom row shows anomalies from the regional mean. Here SPCZ area is averaged over all days from November to April 1980–2012 giving a mean value for each 3 h observational time. The same is done for IR temperature after first averaging the IR temperature spatially within the SPCZ label. Figures 2a and 2b highlight major differences between the regions, while Figures 2c and 2d emphasize the diurnal cycle characteristics. For example, the clouds that make up the tropical part of the SPCZ in the west tend to be deeper (cooler IR temperatures) and cover more area than the clouds that make up the SPCZ further east and between 15°S and 30°S, shown in Figures 2a and 2b.

Despite large differences between regions in the overall mean area, the anomalies are quite similar except for Region 1 where numerous islands are located as discussed above. Maximum area occurs between 15:00 and 18:00 LST in all regions when area is between 10 and 21% greater than the mean. With the exception of the easternmost and westernmost regions, minimum area occurs between 05:00 and 09:00 LST, during which

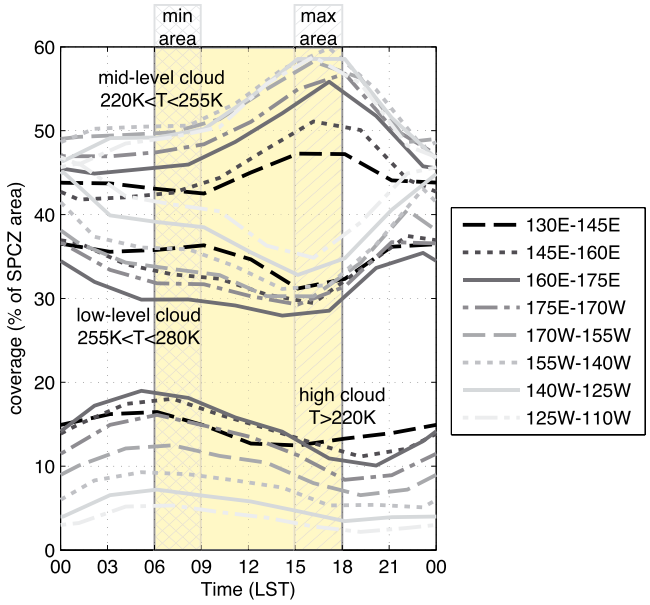

Figure 3. Diurnal cycle of various cloud types within SPCZ (% of SPCZ area) for each subregion. Minimum SPCZ area and maximum SPCZ area are also indicated with hash marks. Yellow shading approximates daylight hours within the diurnal cycle.

time the area is between 7 and 11% below the mean value. In the easternmost region, where the SPCZ is located near 30°S, the minimum in area occurs between 01:00 and 02:00 LST. The diurnal cycle of the SPCZ in the westernmost region, which is partially over land, reaches a lower minimum area at a later time, between 09:00 and 12:00 LST. The amplitude of the diurnal cycle in area is smaller in western, tropical regions and larger for eastern regions where the SPCZ is located in the subtropics. This contradicts previous work such as *Fu et al.* [1990], which notes that the diurnal cycle is strongest where convection is strongest. However, their study focused on the tropics only, whereas the SPCZ reaches into the subtropics.

Figure 2b demonstrates the difference in mean IR temperature within SPCZ labels in the different regions. The mean IR temperature is an average over all cloud types within the SPCZ label. In general, cooler mean IR temperature is associated with a greater number of high clouds, while a warmer mean IR temperature is associated with more clear sky and lower clouds. The phase of the diurnal cycle in terms of mean IR temperature is different for the different regions, which was not the case for SPCZ area. All regions have a double minimum in IR temperature, one occurring in the morning and one occurring in the afternoon. In the western regions (2–4, within the tropics) the primary minimum in IR temperature occurs in the early morning between 05:00 and 07:00 LST. In the eastern regions (5–8, where the SPCZ is more subtropical) the primary minimum in IR temperature occurs in the afternoon between 13:00 and 16:00 LST. The double peak is more obvious in Figure 2d, which shows anomalies from the mean. In the summer east Pacific Intertropical Convergence Zone (ITCZ) *Bain et al.* [2010] found that between 90°W and 120°W the minimum in IR temperature occurs in the afternoon while farther west, between 150°W and 180°W it occurs both in the morning and afternoon. While we also find that the morning peak becomes more prominent farther west, our analysis is complicated by the diagonal tilt of the SPCZ and the deviation of the cloud band away from the equator toward the east. Again, Region 1 has a unique diurnal cycle with a maximum IR temperature occurring at 12:00 LST and a secondary maximum occurring at 21:00 LST (Figures 2b and 2d). Similar to area, we find that the amplitude of the diurnal cycle in terms of mean IR temperature is larger in the subtopics than in the tropics when we examine the IR temperature anomalies or subtract the mean IR temperature for the region at each time (Figure 2d).

To help clarify the regional differences in the phase of the diurnal cycle the distribution of IR temperature within the SPCZ labels has been deconstructed into four categories to represent different cloud heights: high clouds ($IR < 220$ K), midlevel clouds ($220\ K < IR < 255$ K), low-level clouds ($255\ K < IR < 280$ K), and clear sky ($IR > 280$ K). The diurnal cycle of high, low-level, and midlevel clouds is shown in Figure 3, which also indicates the timing of the diurnal cycle of SPCZ area. This result is presented with the caveat that at the pixel level ($0.5° \times 0.5°$) a distinction cannot be made for overlapping clouds. Midlevel clouds cover the largest percentage of the SPCZ in all regions at all times, on average covering between 40% and 60% of the area. The subtropical parts of the SPCZ have a higher percentage of midlevel clouds than the tropical parts of the SPCZ. Low-level clouds are the next most abundant, covering between 28% and 48% of the SPCZ area depending on the time of day and region. Again, the subtropical SPCZ has a higher percentage of low-level clouds than the tropical SPCZ. High-level clouds cover between 2% and 20% of SPCZ area, and the tropical SPCZ has a higher percentage of high-level clouds. To summarize, the tropical SPCZ contains the highest percentage of high clouds while the subtropical SPCZ contains the highest percentage of midlevel and low-level clouds.

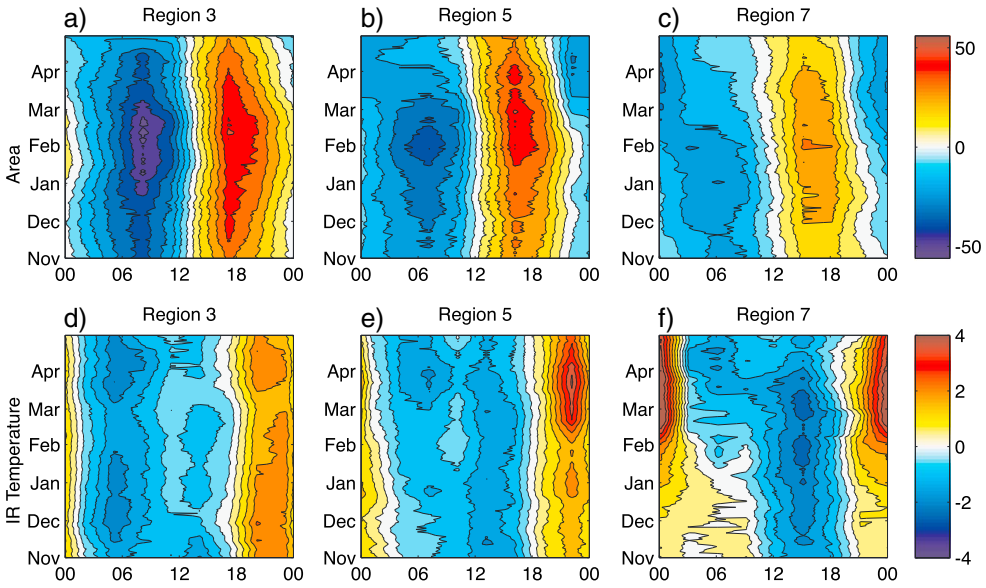

Figure 4. The top row shows (a–c) the seasonal change in the diurnal cycle in terms of anomalies in mean area (number of 0.5° pixels, each region is of equal total area) for regions 3, 5, and 7, respectively. The bottom row shows (d–f) the same for anomalies in mean IR temperature (K).

Each cloud type peaks at a different point in the diurnal cycle, indicating a preference for different convection types at different times of the day. At the beginning of the diurnal cycle at 00:00 LST, low-level clouds are at a maximum and this peak has been building since the 15:00 LST the previous day. After midnight the abundance of low-level clouds lessens and the percent of high-level clouds begins to increase. During this time there is little change in midlevel clouds, indicating a quick transition from low-level to high-level clouds in the early morning hours. *Bain et al.* [2010] found the same quick transition from low-level to high-level clouds in the early morning hours in the summer east Pacific ITCZ. Some studies suggest that an early morning peak in deep clouds over the ocean could be due to cloud top radiative cooling causing instability and increased convection [e.g., *Yang and Slingo*, 2001] and the quick transition from low to high-level clouds supports this hypothesis. The abundance of high-level clouds peaks between 03:00 and 06:00 LST. This corresponds to a time when the overall SPCZ area is at a minimum. By late afternoon when SPCZ area is at a maximum (15:00–18:00 LST), midlevel clouds have reached maximum coverage (15:00–18:00) and low-level clouds are at a minimum (14:00–16:00 LST). High-level clouds reach a minimum area between 18:00 and 21:00 LST.

This analysis clarifies that the morning minimum in mean IR temperature is due to an increase in deep clouds. In subtropical regions the morning minimum is the secondary peak in cloudiness because there are fewer deep clouds in the eastern, subtropical SPCZ. The afternoon minimum mean IR temperature occurs just before the peak in midlevel clouds and during maximum SPCZ area and is the time when there is a balance between a shrinking number of deep cold clouds and growing number of midlevel clouds. Again, this is consistent with the results for the east Pacific ITCZ [*Bain et al.*, 2010].

3.2. Seasonal Changes to the Diurnal Cycle in SPCZ Area and Mean IR

Kikuchi and Wang [2008] show differences in the diurnal cycle of TRMM rainfall between the austral winter (June-July-August) and summer seasons (December-January-February), and *Nitta and Sekine* [1994] show changes to the diurnal cycle in cold clouds ($<$250 K) over the entire year, but only at four locations. To our knowledge there has not been a comprehensive study to date on the detailed evolution of the diurnal cycle from November to April and how the evolution differs for different parts of the SPCZ.

To address this, three of the eight regions described above have been chosen to represent different segments of the SPCZ. Region 3 is used for the tropical, western portion of the SPCZ; Region 5 is used for the transition, or central portion of the SPCZ; and Region 7 is used for the subtropical, eastern portion of the SPCZ. *Haffke and Magnusdottir* [2013] show that the tropical and subtropical parts of the SPCZ have

different seasonal cycles in terms of area and activity (fraction of time present). The subtropical SPCZ is most frequently present in November and December and least frequently present in March, while the tropical SPCZ is frequently active in January and February and least active in November. The same is true for the SPCZ area. Due to these differences, one might expect the amplitude or timing of the diurnal cycle to change throughout the SPCZ active season and not necessarily change in the same way for all parts of the SPCZ. Figure 4 shows how this seasonal variability in SPCZ activity impacts the diurnal cycle in mean IR temperature and area for the three regions of the SPCZ. In Figure 4, time of year is labeled by months from November to April on the vertical axis and increases toward the top while LST is plotted on the horizontal axis and increases toward the right.

Figure 2c shows that when averaged over the season, the tropical SPCZ (Region 3, solid bold contour) reaches maximum area around 17:00 LST, minimum area around 08:00 LST. When the diurnal cycle in area is examined throughout the SPCZ active season we find that the phase is the same, but the amplitude changes over this time period (Figure 4a). The largest amplitude in area during the diurnal cycle occurs in mid-February. In terms of mean IR temperature Figure 2b shows that on average over November–April, a maximum in IR temperature occurs around 20:00 LST while the primary minimum occurs around 05:00 LST, when the largest percentage of deep cloud coverage is reported (Figure 3). The secondary minimum in IR temperature occurs around 14:00 LST as mid-level clouds are increasing. Figure 4d indicates how this pattern changes from November to April. The tropical segment of the SPCZ has a double peak in cloud height (minimum IR temperatures) for much of the season but the secondary, early afternoon IR temperature minimum is much weaker late in the season in March–April while the afternoon peak actually dominates in early Nov (Figure 4d). The timing of the minimum and maximum IR temperature does not change from November to April.

In the central/transition segment of the SPCZ (Region 5; Figure 4b), area peaks near 16:00 LST both in the seasonal mean and at all times of the season. The minimum area occurs around 07:00 LST on average, but the exact timing changes throughout the season. From November to early March the minimum area occurs at 07:00 LST but in March and April it occurs much earlier, around 22:00 LST the day before. The amplitude of the diurnal cycle in area peaks in February, similar to the tropical region. In terms of IR temperature (Figure 4e), on average a minimum occurs around 13:00 LST and a secondary minimum occurs around 07:00 LST. However, we find that the double minimum in IR temperature only begins to occur in late December, continuing through the remainder of the season. Only the afternoon peak is evident before late December. In this segment of the SPCZ, characteristics of both the tropical and subtropical SPCZ can be identified. By late March, the magnitude of the double peak in cold clouds is nearly equal, indicating a mix of the tropical, morning-dominated IR temperature minimum and the subtropical, afternoon-dominated IR temperature minimum. In the beginning of the season this transition region has diurnal cycle characteristics more similar to the subtropical region; in that the afternoon IR temperature minimum is the only peak in cold clouds.

In the subtropical part of the SPCZ (Region 7) the maximum SPCZ area occurs at 15:00 LST, on average, and the minimum at 06:00 LST, according to Figure 2c. In Figure 4c maximum SPCZ area indeed occurs around this time throughout the season; however, a shift in the timing of minimum area occurs. From November to mid-January area minimum occurs around 06:00 LST, from mid-January to mid- February the minimum occurs early, around 03:00 LST, then from mid-February through the remainder of the season the minimum occurs around midnight LST (Figure 4c). This is the largest seasonal change in the phase of the diurnal cycle from all three regions. In terms of IR, a strong peak in deep cloud cover occurs in the afternoon, peaking near 15:00 LST during all months and a secondary peak in deep cloud cover occurs around 06:00 LST starting in mid-January.

In summary, we find that the seasonal cycle has a small impact on the timing of the diurnal cycle in area, in most regions. The only region where it matters is in the subtropics late in the season. Throughout the season, the amplitude of the diurnal cycle in mean IR temperature can change, sometimes resulting in the timing of minimum IR temperature to switch between morning and afternoon. This implies that the phase of the diurnal cycle in IR temperature depends on the months being averaged.

3.3. Modulation of the SPCZ Diurnal Cycle During MJO Events

The MJO is a dominant mode of intraseasonal variability in the tropical Pacific [*Madden and Julian*, 1972]. Past studies have indicated that the diurnal cycle is modulated by the MJO by either increasing [*Chen and*

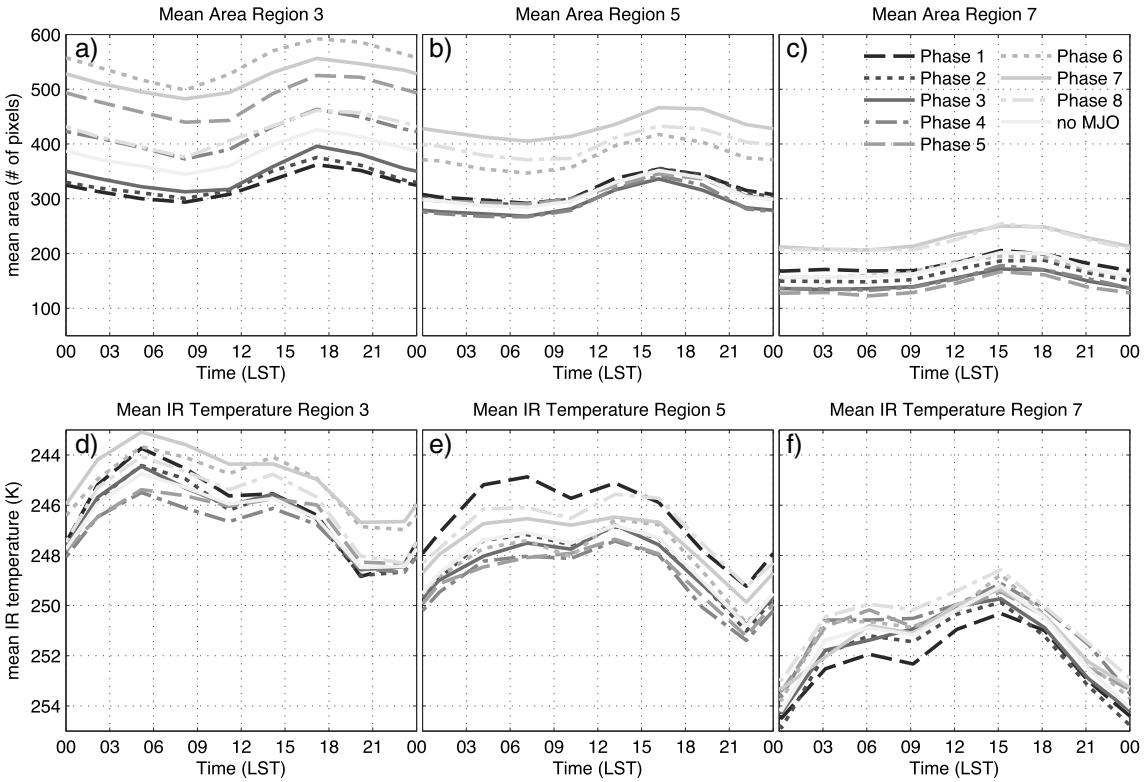

Figure 5. Panels in the top row show changes to the diurnal cycle of (a–c) mean SPCZ area (number of 0.5° pixels) between different phases of the MJO for regions 3, 5, and 7, respectively. Bottom row shows the same for (d–f) mean IR temperature (K).

Houze, 1997; *Tian et al.*, 2006; *Peatman et al.*, 2013; *Oh et al.*, 2012] or decreasing [*Sui and Lau*, 1992] the strength of the diurnal cycle. To further explore this, the diurnal cycle in Regions 3, 5, and 7 will be examined in detail during different phases of the MJO. Note that Region 1 (Maritime continent) is not included in our discussion of MJO events and the diurnal cycle. Here we will use the MJO phases described in *Wheeler and Hendon* [2004]. As in the analysis in *Haffke and Magnusdottir* [2013] only days with a strong MJO signal are considered so we require that the MJO index has an amplitude greater than 1.

Haffke and Magnusdottir [2013] show how SPCZ activity (in terms of fraction of time present) changes during each phase of the MJO (see their Figure 8) by compositing SPCZ labels by MJO phase. When the MJO is initiated in the Indian Ocean, subsidence occurs over the maritime continent and western Pacific (phases 2 and 3), suppressing SPCZ activity. The MJO then passes over the maritime continent (phases 4 and 5) causing enhanced SPCZ activity over New Guinea and suppressed convection directly to the east near the equator, resulting in a poleward shift in SPCZ location. The poleward shift may be enhanced by an increase in easterly winds to the west of the suppressed portion of the SPCZ, enhancing convergence to the west. During MJO phases 6 and 7 the convectively active part of the MJO moves over the west Pacific and SPCZ activity is enhanced. Finally, in phases 8 and 1 SPCZ activity is enhanced near the equator in the central Pacific and suppressed over New Guinea and further poleward resulting in an equatorward shift in SPCZ location. To summarize, the behavior of the SPCZ can be sorted into four categories: (1) suppressed SPCZ during MJO phases 2 and 3, (2) a poleward shifted SPCZ during MJO phases 4 and 5, (3) an enhanced SPCZ during MJO phases 6 and 7, and (4) an equatorward shifted SPCZ during MJO phases 8 and 1.

By composite analysis, we find that the magnitude of the peaks in SPCZ area and mean IR temperature changes during an active MJO and in specific ways for each MJO phase. This is shown in Figure 5 indicating the diurnal cycle of area and mean IR temperature for regions 3, 5, and 7 during all MJO phases. In Region 3 (Figures 5a and 5d), the morning and afternoon minimum in IR temperature and the peak in SPCZ area are all largest during MJO phases 6 and 7 when SPCZ activity is enhanced everywhere. In contrast the warmest cloud peaks in this region occur during MJO phases 4 and 5 when the SPCZ tends to shift poleward.

A composite of cloud height by MJO phase in this region (not shown) confirms that deep convection is most active in MJO phase 7 and least active in phases 4 and 5. We noted earlier that during phases 4 and 5 the SPCZ tends to be located further poleward, supporting the idea of more midlevel clouds at the expense of deep convection. Conversely, during phases 8 and 1 the SPCZ is shifted equatorward, while during phase 7 the SPCZ is enhanced, all suggesting that the occurrence of high-level clouds may increase as the SPCZ moves toward the equator and is therefore more active. The smallest peak in SPCZ area occurs in MJO phase 1, when much of the SPCZ is shifted equatorward but the SPCZ in Region 3 is suppressed, and phases 2 and 3 when most of the SPCZ is suppressed. The afternoon peak in SPCZ area is 1.6 times greater in MJO phase 6 than in MJO phase 1.

In Region 5 (Figures 5b and 5e) the SPCZ reaction to an MJO event is slightly delayed compared to Region 3. In Region 5 the SPCZ area peaks are the greatest in MJO phases 7, when the SPCZ is enhanced, and phase 8, when the SPCZ shifts equatorward. In terms of minimum IR, the greatest minimum is observed during MJO phases 1 and 8 when the SPCZ is shifted equatorward. During phases 1, 8, and 7 the morning and afternoon IR temperature minimums are nearly equal in magnitude and in phase 1 the morning peak dominates. During all other times the afternoon IR temperature minimum is larger in amplitude. The equatorward shift means that the SPCZ is located over warmer SSTs, allowing for the development of deeper convection. In contrast the warmest IR temperature minimums occur in MJO phases 4 and 5 when the SPCZ shifts poleward, away from warm SST. The smallest peak in area occurs in MJO phase 3 when the SPCZ is suppressed. During phase 7 the peak in area is 1.4 times larger.

Region 7 (Figures 5d and 5f) is of smaller area at all times compared to the other two regions. The morning and afternoon IR temperature minima are strongest during MJO phase 8 but weakest just a short time later in phase 1. The area of the SPCZ in Region 7 is much smaller than in regions 3 and 5. SPCZ area has the largest peak during MJO phases 7 and 8 when it is 1.4 times larger than in phase 5 when the peak is the smallest.

These results agree well with *Tian et al.* [2006], which found that the diurnal cycle of deep convective clouds was amplified during the active convective phases of the MJO and suppressed during the suppressed phases of the MJO without a change in the phase of the diurnal cycle. *Sui and Lau* [1992] found the opposite result or that the diurnal cycle diminished during the active MJO phase and was enhanced during the suppressed phase. Similar to *Chen and Houze* [1997], we find a tendency for the morning peak in cloudiness to occur with the active phase of the MJO. All studies that specifically looked at the modulation of the diurnal cycle by the MJO looked in the tropics, north of 20°S. To the best of our knowledge, ours is the only analysis of changes to the subtropical part of the SPCZ.

3.4. Impact of ENSO on the Amplitude of the SPCZ Diurnal Cycle

Section 3.2 highlighted the changes in the diurnal cycle of SPCZ area and average IR temperature that take place from November to April. Here we will use the same methodology but look at El Niño, La Niña, and ENSO neutral years separately and examine mean IR temperature. The Multivariate ENSO Index (MEI) is used to define the state of ENSO [*Wolter and Timlin*, 1998]. The ENSO state for each SPCZ active season is determined based on the average MEI value over the November/December, December/January, January/February, February/March, and March/April bimonthly periods. The average MEI value determines which season is considered El Niño (MEI $>$ 0.5), La Niña (MEI $<$ $-$0.5), or ENSO neutral ($-0.5 <$ MEI < 0.5). Based on this categorization El Niño years include 1982, 1986, 1987, 1991, 1992, 1994, 1997, 2002, 2004, and 2009, La Niña years include 1984, 1988, 1995, 1998, 1999, 2000, 2005, 2007, 2008, 2010, and 2011, and ENSO neutral years include 1980, 1981, 1983, 1985, 1989, 1990, 1993, 1996, 2001, 2003, and 2006 for a total of 10 El Niño years, 11 La Niña years, and 11 neutral years.

During El Niño years the SPCZ average position typically shifts equatorward and becomes more zonal, while during La Niña years it shifts poleward [*Folland et al.*, 2002; *Vincent et al.*, 2011; *Haffke and Magnusdottir*, 2013]. The goal of this section is to determine whether the diurnal cycle of the SPCZ in terms of IR temperature changes during El Niño and La Niña events, potentially due to a shifted SPCZ location. To retain the seasonal information, diagrams are shown indicating the diurnal cycle as a function of time of season, similar to Figure 4, as a composite of El Niño years (Figures 6a–6c), ENSO neutral years (Figures 6d–6f), and La Niña years (Figures 6g–6i). Again, we focus on the three regions discussed previously, Region 3, Region 5, and Region 7.

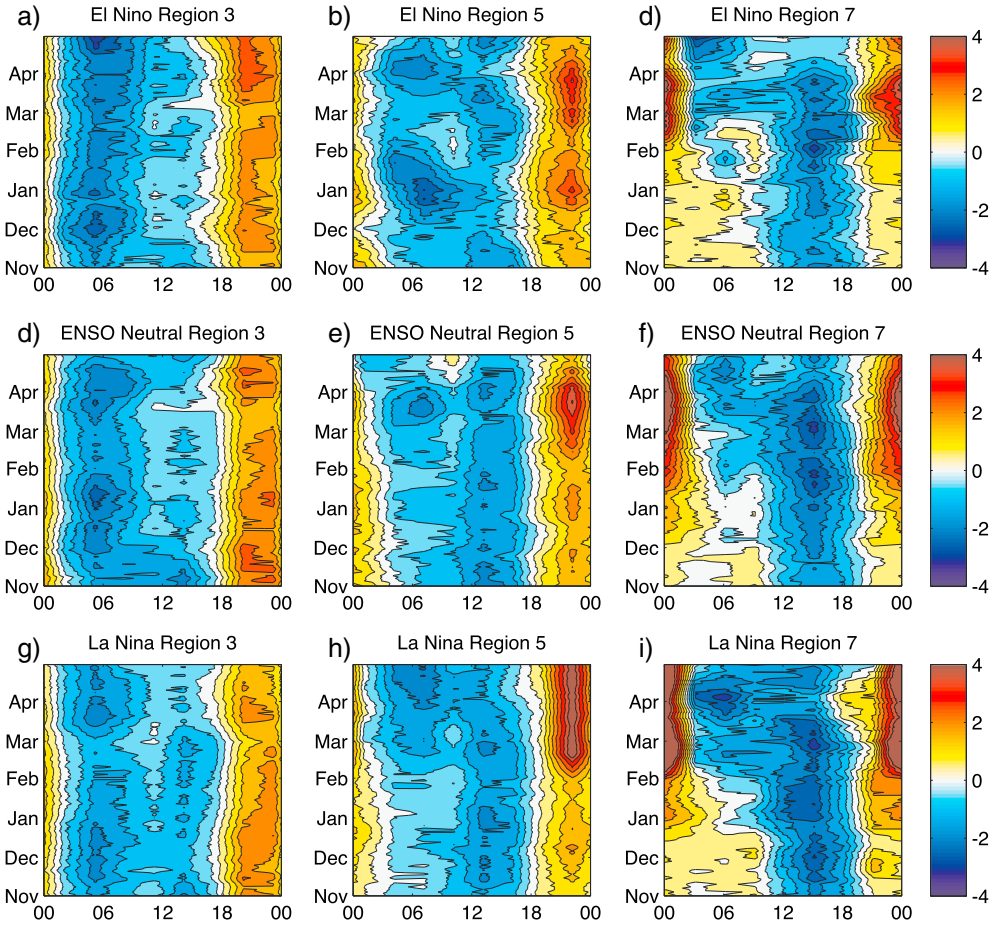

Figure 6. Each panel shows seasonal changes to the diurnal cycle in terms of anomalies of mean IR temperature (K) during (a–c) El Niño years, (d–f) ENSO neutral years, and (g–i) La Niña years for regions 3, 5, and 7.

We find that, depending on the region, the timing of minimum IR temperature is different in El Niño, La Niña, and ENSO neutral years. In Region 3 during neutral or El Niño years, the morning minimum IR temperature is either the only IR temperature minimum throughout the day or it is the stronger of the two minima. However, in La Niña years the afternoon minimum in IR temperature is also strong, particularly from late January to early March. During these years the diurnal cycle in mean IR temperature in the tropical part of the SPCZ looks more like the pattern typically seen in Region 7 as the SPCZ shifts away from the equator.

The diurnal cycle of the SPCZ in Region 7 also supports this argument. The morning minimum is the weaker of the two or does not exist during neutral years, but it is evident in El Niño years. The morning minimum is more characteristic of the tropical regions of the SPCZ and so we see the subtropical SPCZ taking on tropical characteristics during El Niño years, when it shifts equatorward.

4. Conclusions

Here we use a unique data set to quantify the diurnal cycle of SPCZ area, mean IR temperature, and cloud height distribution. The data set spans the months of November–April and includes the years 1980–2012. We split the SPCZ into eight regions to correct for local standard time and to study how the different parts of the SPCZ may differ in terms of the diurnal cycle. We find that almost the entire SPCZ (except Regions 1 and 8) has a distinct diurnal cycle in area and mean IR temperature such that it contracts in area at night and becomes deeper with a minimum area and mean IR temperature in the early morning at 06:00–09:00 LST. We find a quick transition form low-level cloud to high clouds in the early morning hours. The percentage of low-level clouds peaks just before midnight and the peak in deep clouds occurs between 05:00 and 07:00 LST. The transition from low-level

to deep clouds is relatively fast, and between 00:00 and 05:00 LST the percentage of midlevel clouds is not changing. This supports the hypothesis that the atmosphere destabilizes during this time due to radiative cooling resulting in a quick transition from low-level to deep clouds [*Yang and Slingo*, 2001; *Randall et al.*, 1991]. The SPCZ expands during the day with a maximum area in the late afternoon at 15:00–18:00 LST when there is another minimum in mean IR temperature that is mostly due to an increase in midlevel clouds.

The more tropical SPCZ (to the west) has the dominant minimum in IR temperature in the morning between 05:00 and 07:00 LST, while the more subtropical SPCZ has the dominant minimum in the afternoon between 13:00 and 16:00 LST. *Albright et al.* [1985] also noted that the eastern, subtropical SPCZ has an afternoon peak in mean IR. However, they find that the western SPCZ has a peak in mean IR temperature in the late evening hours, around 21:00 LST, which is inconsistent with out results. Our results largely agree with those presented in *Nitta and Sekine* [1994] that indicate a morning peak between 03:00 and 04:00 LST (our early morning peak occurs slightly later) and a secondary peak between 15:00 and 16:00 LST.

We find that the timing of the diurnal cycle is consistent throughout the austral summer half year in the tropics, especially in terms of SPCZ area. More variability between the beginning of the season, height of the season, and end of the season are seen in the central part of the SPCZ, where it transitions from a tropical convection zone to a more subtropical type convection zone. In the central and subtropical parts of the SPCZ the timing of the minimum area tends to shift to earlier hours of the morning, or even before midnight, later in the season. In all regions there tends to be a double minimum in IR temperature, a morning peak associated with a maximum in high clouds, and an afternoon peak associated with an increase in midlevel clouds. However, in November–January we find that only the afternoon minimum IR temperature occurs in the transition regions or subtropical regions. This seems to indicate that the more subtropical parts of the SPCZ tend to start behaving more like the tropical SPCZ only after January even though this is when the subtropical SPCZ tends to be less active compared to the beginning of the season.

We find that the MJO and ENSO modify the diurnal cycle of mean IR temperature in the SPCZ similarly: when the SPCZ shifts equatorward, either during an El Niño year (due to warm SST in the equatorial area) or during phases 8 and 1 of the MJO, deep clouds tend to cover more area and the morning peak in mean IR temperature dominates. When the SPCZ shifts poleward, either during La Niña or during phases 4 and 5 of the MJO, the afternoon peak in mean IR temperature tends to dominate as the percentage of deep clouds is less. This is particularly apparent in Region 5 where larger north-south shifts in SPCZ position can occur than for other regions. This suggests that the proximity of the SPCZ to the equator is an important factor in determining if the morning minimum in IR temperature is dominant.

Acknowledgments

The authors acknowledge Ken Knapp at NOAA's National Climatic Data Center for providing IR data from the GridSat database. The IR data are available for download from the GridSat database at http://www.ncdc.noaa.gov/gridsat/. The authors thank the anonymous reviewers for helpful comments on the manuscript. This research was supported by NSF grant AGS–1206120.

References

Albright, M. D., E. E. Recker, R. J. Reed, and R. Dang (1985), The diurnal variation of deep convection and inferred precipitation in the central tropical Pacific during January–February 1979, *Mon. Weather Rev.*, *113*, 1663–1680.

Bain, C. L., G. Magnusdottir, P. Smyth, and H. Stern (2010), Diurnal cycle of the Intertropical Convergence Zone in the east Pacific, *J. Geophys. Res.*, *115*, D23116, doi:10.1029/2010JD014835.

Bain, C. L., J. De Paz, J. Kramer, G. Magnusdottir, P. Smyth, H. Stern, and C.-C. Wang (2011), Detecting the ITCZ in instantaneous satellite data using spatiotemporal statistical modeling: ITCZ climatology in the east Pacific, *J. Clim.*, *24*, 216–230, doi:10.1175/2010JCLI3716.1.

Chen, S. S., and R. A. Houze (1997), Diurnal variation and life-cycle of deep convective systems over the tropical pacific warm pool, *Q. J. R. Meteorol. Soc.*, *123*, 357–388, doi:10.1256/smsqj.53805.

Dai, A. (2001), Global precipitation and thunderstorm frequencies. Part I: Seasonal and interannual variations, *J. Clim.*, *14*, 1092–1111.

Dorman, C. E., and R. H. Bourke (1979), Precipitation over the Pacific Ocean, 30°S to 60°N, *Mon. Weather Rev.*, *107*, 896–910.

Folland, C. K., J. A. Renwick, M. J. Salinger, and A. B. Mullan (2002), Relative influences of the Interdecadal Pacific Oscillation and ENSO on the South Pacific Convergence Zone, *Geophys. Res. Lett.*, *29*(13), 1643, doi:10.1029/2001GL014201.

Fu, R., D. Genio, D. Anthony, and W. B. Rossow (1990), Behavior of deep convective clouds in the tropical Pacific deduced from ISCCP radiances, *J. Clim.*, *3*, 1129–1152.

Gray, W. M., and R. W. Jacobson (1977), Diurnal variation of deep cumulus convection, *Mon. Weather Rev.*, *105*, 1171–1188.

Haffke, C., and G. Magnusdottir (2013), The South Pacific Convergence Zone in three decades of satellite images, *J. Geophys. Res. Atmos.*, *118*, 10,839–10,849, doi:10.1002/jgrd.50838.

Janowiak, J. E., P. A. Arkin, and M. Morrissey (1994), An examination of the diurnal cycle in oceanic tropical rainfall using satellite and in situ data, *Mon. Weather Rev.*, *122*, 2296–2311.

Kikuchi, K., and B. Wang (2008), Diurnal precipitation regimes in the global tropics, *J. Clim.*, *21*, 2680–2696, doi:10.1175/2007JCLI2051.1.

Knapp, K. R., et al. (2011), Globally Gridded Satellite observations for climate studies, *Bull. Am. Meteorol. Soc.*, *92*, 893–907, doi:10.1175/2011BAMS3039.1.

Madden, R. A., and P. R. Julian (1972), Description of global-scale circulation cells in the tropics with a 40–50 day period, *J. Atmos. Sci.*, *29*, 1109–1123.

Matthews, A. J. (2012), A multiscale framework for the origin and variability of the South Pacific Convergence Zone, *Q. J. R. Meteorol. Soc.*, *138*, 1165–1178, doi:10.1002/qj.1870.

Meisner, B. N., and P. A. Arkin (1987), Spatial and annual variations in the diurnal cycle of large-scale tropical convective cloudiness and precipitation, *Mon. Weather Rev.*, *115*, 2009–2032.
Nesbitt, S. W., and E. J. Zipser (2003), The diurnal cycle of rainfall and convective intensity according to three years of TRMM measurements, *J. Clim.*, *16*, 1456–1475, doi:10.1175/1520-0442-16.10.1456.
Nitta, T., and S. Sekine (1994), Diurnal variation of convective activity over the tropical western Pacific, *J. Meteorol. Soc. Jpn.*, *72*(5), 627–641.
Oh, J.-H., K.-Y. Kim, and G.-H. Lim (2012), Impact of MJO on the diurnal cycle of rainfall over the western Maritime continent in the austral summer, *Clim. Dyn.*, *38*, 1167–1180, doi:10.1007/s00382-011-1237-4.
Peatman, S. C., A. J. Matthews, and D. P. Stevens (2013), Propagation of the Madden-Julian Oscillation through the Maritime Continent and scale interaction with the diurnal cycle of precipitation, *Q. J. R. Meteorol. Soc.*, *140*, 814–825, doi:10.1002/qj.2161.
Randall, D. A., D. A. Dazlich, and Harshvardhan (1991), Diurnal variability of the hydrologic cycle in a general circulation model, *J. Atmos. Sci.*, *48*(1), 40–62.
Sui, C.-H., and K.-M. Lau (1992), Multiscale phenomena in the tropical atmosphere over the western Pacific, *Mon. Weather Rev.*, *120*, 407–430.
Takahashi, K., and D. S. Battisti (2007), Processes controlling the mean tropical Pacific precipitation pattern. Part II: The SPCZ and the Southeast Pacific dry zone, *J. Clim.*, *20*(23), 5696, doi:10.1175/2007JCLI1656.1.
Teo, C.-K., T.-Y. Koh, J. C.-F. Lo, and B. C. Bhatt (2011), Principal component analysis of observed and modeled diurnal rainfall in the maritime continent, *J. Clim.*, *24*, 4662–4675, doi:10.1175/2011JCLI4047.1.
Tian, B., D. E. Waliser, and E. J. Fetzer (2006), Modulation of the diurnal cycle of tropical deep convective clouds by the MJO, *Geophys. Res. Lett.*, *33*, L20704, doi:10.1029/2006GL027752.
Vincent, D. G. (1994), The South Pacific Convergence Zone (SPCZ): A review, *Mon. Weather Rev.*, *122*, 1949–1970.
Vincent, E. M., M. Lengaigne, C. E. Menkes, N. C. Jourdain, P. Marchesiello, and G. Madec (2011), Interannual variability of the South Pacific Convergence Zone and implications for tropical cyclone genesis, *Clim. Dyn.*, *36*(9–10), 1881–1896, doi:10.1007/s00382-009-0716-3.
Wheeler, M. C., and H. H. Hendon (2004), An all-season real-time multivariate MJO index: Development of an index for monitoring and prediction, *Mon. Weather Rev.*, *132*, 1917–1932.
Widlansky, M. J., P. J. Webster, and C. D. Hoyos (2011), On the location and orientation of the South Pacific Convergence Zone, *Clim. Dyn.*, *36*, 561–578, doi:10.1007/s00382-010-0871-6.
Wolter, K., and M. S. Timlin (1998), Measuring the strength of ENSO events: How does 1997/98 rank?, *Weather*, *53*, 315–324.
Yang, G. Y., and J. Slingo (2001), The diurnal cycle in the tropics, *Mon. Weather Rev.*, *129*, 784–801.
Yang, S., and E. A. Smith (2006), Mechanisms for diurnal variability of global tropical rainfall observed from TRMM, *J. Clim.*, *19*, 5190–5226.
Yen, M. C. (2005), Interannual variation of the diurnal convection cycle in the western North Pacific, *Meteorol. Atmos. Phys.*, *90*, 67–75, doi:10.1007/s00703-004-0104-9.